

DIAGNOSTIC CASE REPORT

U. S. GEOLOGICAL SURVEY-BIOLOGICAL RESOURCES DIVISION
 NATIONAL WILDLIFE HEALTH CENTER-HONOLULU FIELD STATION
 P. O. BOX 50167, 300 ALA MOANA BLVD., Rm. 8-132
 HONOLULU, HAWAII 96850
 Tel: 808-792-9520, Fax: 792-9596, Email: thierry_work@usgs.gov

Case: 25721

Submitter:

Dr. Jan Landsberg
 Florida Fish and Wildlife Conservation
 Commission
 100 Eighth Ave SE
 St. Petersburg, Florida 33701
 United States

Species submitted (n)

Coral: *Colophyllia natans* (5)
 Coral: *Montastraea cavernosa* (6)
 Coral: *Orbicella faveolata* (5)
 Coral: *Pseudodiploria strigosa* (6)
 Coral: *Siderastrea siderea* (5)

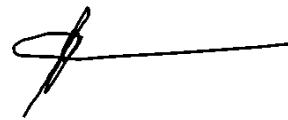
SPECIMENS SUBMITTED: Tissues fixed

Executive summary: Stony coral tissue loss disease (SCTLD) was first documented in 2014 near Miami harbor Florida and has since spread north and south along the Florida reef tract killing large numbers of at least 19 species of corals and leading to the functional extinction of at least one species, *Dendrogyra cylindricus*. SCTLD is assumed to be caused by bacteria based on presence of different assemblages of bacteria in lesioned vs normal tissues, its apparent spread among colonies, and cessation of spread of lesions in individual colonies treated with antibiotic paste. However, microscopic examination of tissues of corals affected with SCTLD have not revealed the presence of bacteria associated with tissue death. Rather, microscopic evidence of dead and dying coral cells and Symbiodiniaceae, historically and colloquially called Zooxanthellae, in colonies affected with SCTLD suggests a breakdown of host cell/Zooxanthellae symbiosis. It is unclear whether host cells die first leading to death of Zooxanthellae or vice versa. Based on microscopy, hypotheses as to possible causes of SCTLD include infectious agents not visible at the light microscopy level or some sort of toxicosis, perhaps originating from Zooxanthellae. To clarify this, we examined corals affected with SCTLD using electron microscopy which permits visualization of details not visible on light microscopy. Here we show that Zooxanthellae in SCTLD-affected corals consistently manifest varying degrees of pathology associated with elongated particles compatible in morphology with filamentous single stranded RNA viruses of plants (anisometric viral like particles-AVLP). Our findings showed what appeared to be a progression from early to late replication of AVLP in chloroplasts with little to no coral host cell pathology other than cell lysis. In addition to AVLP, Zooxanthellae showed pathology in chloroplasts consistent with that seen in plants infected by viruses. Based on these findings, we hypothesize that SCTLD is a viral disease of Zooxanthellae leading to coral host death. Efforts to confirm the presence of a virus associated with SCTLD through other means should be a priority. These include showing the presence of a virus through molecular assays such as deep sequencing, attempts to grow this virus in the laboratory through culture of Zooxanthellae, localization of virus in tissue sections using immunohistochemistry or in-situ hybridization, and experimental infection of known-virus-negative corals to replicate disease at the gross and microscopic level.

Details of the findings above are in the attached report.

Report Date (mm/dd/yyyy): 06/15/2021 **Necropsy report:** Attached

Copies of this report sent to:

A handwritten signature in black ink, consisting of a stylized, cursive initial followed by a long horizontal line extending to the right.

If you have questions regarding this case, contact Thierry M. Work MS, DVM, MPVM at 808-792-9520. Include above Case Number. Diagnostic findings may not be used for publication without the pathologist's knowledge and consent.

Final report on electron microscopy of Florida corals affected with stony coral tissue loss disease (SCTLD).

Final report to the Florida Department of Environmental Protection and the Florida Fish & Wildlife Conservation Commission

Thierry M. Work, Wildlife Disease Specialist, U.S. Geological Survey, National Wildlife Health Center, Honolulu Field Station, PO Box 50187, Honolulu, HI 96850. Tel: 808 792 9520. Email: thierry_work@usgs.gov.

1. Background:

Stony coral tissue loss disease (SCTLD) was first identified in 2014 near Miami Florida (Precht et al. 2016) and has since appeared in other parts of the Caribbean. The disease presents as varying degrees of acute to subacute tissue loss affecting at least 19 species of corals and is assumed to be caused by an infectious agent (Muller et al. 2020). Supporting this conjecture is a spatial epidemiology suggestive of a contagion (Muller et al. 2020), corals affected to SCTLD have particular clades of bacteria associated with lesions (Rosales et al. 2020), and affected corals respond positively to treatments with antibiotics (Neely et al. 2020) although this practice does not prevent genesis of additional lesions (Shilling et al. 2021).

Contradicting the possibility that bacteria cause SCTLD are light microscopy descriptions of the disease that have, to date, not shown bacteria or any other organism associated with cell pathology. Rather, histopathology indicates that SCTLD appears to be a dysfunction of host-Zooxanthellae symbiosis leading to death of Zooxanthellae, historically and colloquially called Zooxanthellae, and host cells resulting in gross clinical signs of tissue loss. Based on microscopic findings, the hypothesis is that either Zooxanthellae are dying leading to host cell death or vice versa. Because light microscopy cannot, in general, resolve microorganisms smaller than bacteria, SCTLD could be caused by smaller infectious agents such as viruses. Alternatively, SCTLD could be some sort of toxicosis that leads to host cells (Landsberg et al. 2020). For instance, dinoflagellates are known to produce a host of toxic substances that can be harmful to humans and fish (Glibert and Burkholder 2018), so plausibly, Zooxanthellae might be producing toxins that kill the coral host.

Transmission electron microscopy can complement light microscopy by revealing details at the subcellular level not visible on light microscopy (ultrastructure). For instance, electron microscopy allows for detection of very small structures like cell organelles and viruses. The purpose of this study was to examine tissues from SCTLD affected corals by electron microscopy to characterize the disease at the ultrastructural level in attempts to clarify whether: 1) The disease process starts with death of Zooxanthellae or death of host cells and 2) infectious agents not visible at the light microscopy level could be associated with cell pathology. Results herein point to SCTLD being a viral infection of Zooxanthellae that leads to coral host cell death.

2. Methods:

Corals were collected from various locations in Florida in electron microscopy fixative as described (Landsberg et al. 2020) from coral colonies from various locations in Florida (Table 1). Fragments were labelled as originating from apparently healthy colonies (Healthy), or colonies manifesting gross lesions of SCTLD comprising apparently normal fragments (SCTLD-Healthy) or fragments with lesions (SCTLD-Lesion).

Fragments were decalcified in EDTA and post fixed in Karnovsky's fixative. Tissues were then rinsed in 0.1 M sodium cacodylate buffer containing 0.35 M sucrose and postfixed with 1% osmium tetroxide in 0.1 M sodium cacodylate buffer. Tissue was dehydrated in a graded ethanol series, the

ethanol was replaced with propylene oxide, and the tissue was embedded in LX112 epoxy resin. Epoxy-embedded tissues were cut into 1 µm thick sections and stained with Richardson's stain for light microscopy. For electron microscopy, ultrathin (60 to 80 nm) sections were obtained on an RMC Powertome ultramicrotome, double stained with uranyl acetate and lead citrate, viewed on a Hitachi HT7700 transmission electron microscope (TEM) at 100 kV, and photographed with an AMT XR-41B 2k-by-2k charge-coupled device (CCD) camera. Cells of surface body wall (epidermis, mesoglea, gastrodermis with Zooxanthellae) and basal body wall (gastrodermis with Zooxanthellae, mesoglea, calicodermis) were examined and representative lesions were photographed. Cells were judged healthy if they had intact cell and nuclear membranes with expected complement of organelles or appropriate structures to that cell type (Harrison and Ruppert 1990).

During examination of tissues, it became evident, based on lack of significant pathology in host cells vs those of Zooxanthellae, that efforts be dedicated to documenting changes in Zooxanthellae. Normal Zooxanthellae (Trench and Blank 1987) are characterized by a cell comprising mainly chloroplasts composed of stacked thylakoid membranes, a pyrenoid surrounded by an annulus of starch, a nucleus, and mitochondria (Fig. 1A). The following features were labelled as 1 if seen or 0 if not: loss of laminar detail in thylakoid membranes, gigantism of chloroplast, absence of starch granules, absence of annular starch around pyrenoid (Fig. 1B), presence of amorphous homogenous electron dense aggregates in cell stroma (Fig. 1C), presence of variably sized cavities within the cell stroma (Fig. 1C-D). We also categorized anisometric viral-like particles (AVLP) compatible in morphology and size with single stranded RNA viruses of plants with linear to sinuous morphology (Stevens 1983, Agrios 2004) as follows: whorled electron dense material (viroplasm) (Fig. 1E) often associated with fine AVLP (Fig. 1F; Fig. 2A-B), coarse AVLP arranged in stellate clusters (Fig. 2C-D), or coarse AVLP in layered or haphazard clusters (Fig. 2E-F). From photographs, we enumerated and plotted for each genus and sample disease state (Healthy, SCTL-Healthy, SCTL-Lesion) percent of Zooxanthellae having these features.

3. Results:

We received 27 samples comprising five species of corals including six samples each from *Montastraea cavernosa*, and *Pseudodiploria strigosa*, and five each from *Colpophyllia natans*, *Orbicella faveolata*, and *Siderastrea siderea* comprising 12 SCTL-Healthy, 10 SCTL-Lesion, and 5 Healthy. Of these, TEM was done on 25 samples; two samples had tissues unsuitable for examination due to decomposition (Table 1).

A total of 1776 electron micrographs were taken from the 25 fragments, and 644 individual Zooxanthellae were photographed (table 2). Of the 10 changes enumerated from photographs, the most common was presence of a cavity within the cell (75%), followed by absence of annular starch around pyrenoid (66%), electron dense material within cell stroma (64%), coarse arrayed in stellate pattern (54%), absence of starch granules (45%), indistinct thylakoid membranes (34%), fine AVLP (20%), coarse AVLP arrayed as lamina or haphazardly (14%), black whorls (viroplasm) (13%), and gigantism of chloroplasts (4%).

3.1 Putative viral infections

Putative early viral infections were characterized by clumps of electron dense whorls associated with fine AVLP (Fig. 1 E-F; Fig. 2A-B). Putative intermediate stage viral infections were characterized by AVLP arrayed in stellate patterns and found almost exclusively in cavities within Zooxanthellae (Fig. 2C-D). Anisometric viral like particles arranged in stellate patterns were occasionally associated with electron dense to stippled viroplasm (Fig. 3A) and more often with stacked or laminated membranes (Fig. 3B). Membranes were also evident associated with stippled viroplasm (3C-D). Putative late stage infections were characterized by large cavities replete with coarse AVLP (Fig. 2E-F) that occasionally

appeared to originate from electron dense viroplasms (Fig. 3E-F). Anisometric viral like particles ranged in diameter from 15-20 nm. Terminal infections were characterized by Zooxanthellae distorted with large cavities replete with stacks of coarse AVLP mixed with membranes (Figs. 4A-B) or clusters of AVLP that appeared to be emerging from host cells associated with lysed cell membrane (Figs. 4C-F). Fine AVLP were generally closely associated with whorled viroplasm and were seen in 20-40% of Zooxanthellae photographed regardless of genus or health status (Fig. 5). Stellate AVLP were found in 40-60% of Zooxanthellae whereas coarse AVLP were seen in 0-40% of Zooxanthellae. There was no clear relationship between health status and presence of these AVLP (Fig. 6).

3.2 Cellular pathology

For all but *Orbicella*, there was a trend of increasing percentage of Zooxanthellae missing starch granules with decline in health state; however, absence of circumpyrrenoid starch annulus affected between 50-80% of Zooxanthellae regardless of health state of genus (Fig. 7).

Presence of variably sized intracellular cavities occurred in between 60-90% of Zooxanthellae regardless of health state or genus. For electron dense structures, these occurred between 10-90% of corals and no evident pattern was seen except for a progressive increase with deteriorating health state for *Colpophyllia* (Fig. 8). Of 410 Zooxanthellae with electron dense amorphous structures, 134 had inclusions exclusively within chloroplasts, 180 had them exclusively within cavities, and 96 had them in both compartments.

Gigantism of chloroplasts was seen in 0-20% of Zooxanthellae mainly in *Siderastrea* and *Montastraea*. No clear pattern was observed for indistinct thylakoid membranes which were seen for all health states and genera at levels ranging from 0-90% (Fig. 9).

4. Discussion:

Ultrastructural morphologic changes in Florida corals affected with SCTLTD seen here were suggestive of a viral infection affecting exclusively Zooxanthellae. Abnormalities in host cells were limited to lysis with no associated foreign organisms. In most cases, host cell enclosing the Zooxanthellae were intact with intact nuclei and expected complement of internal organelles. This suggests that SCTLTD is, fundamentally, a Zooxanthellaer disease that eventually leads to coral host cell death. Notable was the presence of AVLP in Zooxanthellae that contained various amounts of structures compatible in morphology with linear to filamentous single stranded RNA viruses known to infect plants (Agrios 2004). Assuming this is the case, two explanations exist for the different morphologies of AVLP seen here: 1) Zooxanthellae are infected with at least three different types of viruses or 2) This variation in morphology reflects different developmental forms of the same virus. As the most parsimonious explanation, we suspect the second option is more likely. In animals (Netherton et al. 2007) and plants (Yang et al. 2017), virus particle assembly goes through a maturation process involving nucleic acids and proteins that are initially visible as amorphous electron dense masses (viroplasm) from which emerge mature viral particles. This pattern was evident in multiple zooxanthellae from multiple corals (Figs. 1E-F; Figs. 2 A-B; Figs. 3E-F). Moreover, positive single stranded RNA viruses are known to promote membrane proliferation in host cells (Netherton et al. 2007), a feature that was prominently seen associated with stellate AVLP (Figs. 3A-D). The size range of AVLP was within the bounds of other plant viruses with similar morphology (Stevens 1983). We inferred the progression of early vs late stage virus disease based on the size of viral inclusions assuming that smaller inclusions most often associated with viroplasm (assembly components of viruses) were early stages and larger inclusions less often associated with viroplasm were likely later stages (McWhorter 1965).

Morphologic changes in host Zooxanthellae including loss of detail of thylakoid membranes and gigantism of chloroplasts were also compatible with the way these organelles respond to virus infections in plants. In plants, the chloroplast is often targeted by viruses (Zhao et al. 2016, Bhattacharyya and Chakraborty 2018), and virus-infected chloroplasts manifest morphologic changes very similar to those seen in Zooxanthellae here. Given that the chloroplast makes up a considerable volume of the Zooxanthellae, this organelle would seem an inviting target for viral infections. Indeed this appeared to be the case as exemplified by the presence of viral inclusions in Zooxanthellae exclusively in chloroplasts. Other changes seen in Zooxanthellae were less clearly associated with viral infections. Electron dense structure in cavities within Zooxanthellae could have been lipids (Weng et al. 2014) or viroplasm. Cavities in Zooxanthellae were round and often filled with debris but were unlike accumulation bodies. Accumulation bodies in Zooxanthellae, hypothesized to be waste accumulation structures, are normally round and filled with tightly packed electron dense material (Taylor 1968, Zhu et al. 2011). In contrast, in Zooxanthellae examined here, cavities were filled with a mix of debris and electron lucent matrix admixed with AVLP, membranes, and viroplasm. Finally, depletion of starch reserves was commonly seen suggesting depletion of energy reserves or inability of the cell to generate sugars. This would accord with chloroplast pathology which likely resulted in reduced ability of the cell to carry out photosynthesis, a key process needed to generate sugars in Zooxanthellae (Yellowlees et al. 2008). Reduced photosynthesis can lead to starch depletion in Zooxanthellae in other cnidaria. For instance, light starved *Aiptasia* have Zooxanthellae with reduced starch reserves (Muller-Parker et al. 1996).

Viruses have been detected in corals by electron microscopy and molecular assays, and they are thought to play important roles in coral bleaching, stress responses, and microbial turnover (Vega Thurber and Correa 2011). Viral like particles (VLP) have also been extensively documented in Zooxanthellae by electron microscopy both in hospite and culture. For instance, VLP were seen in thylakoids of Zooxanthellae from heat shocked *Anemonia viridis* (Wilson et al. 2001), and VLP were seen in animal tissues of heat shocked *Pavona danai* (Wilson et al. 2005). Various morphologies of VLP were seen in mucus of *Pseudodiploria* and *Acropora* from Australia (Davy and Patten 2007), and water surrounding thermally stressed Zooxanthellae (Davy et al. 2006). Unfortunately, in most of these studies, VLP were sparse making them very difficult to differentiate from similar size and shaped structure that often turn out to be artefacts such as condensed proteins or nucleic acids, a common problem in interpretation of transmission electron micrographs (Ackermann and Tiekotter 2012). Moreover, none of these aforementioned studies showed convincing morphologic evidence of cell pathology associated with viral infection. Ideally, documentation of plausible viral infections in organisms by electron microscopy should illustrate various stages of viral morphogenesis associated with clear evidence of cell pathology with abundant virions (Work et al. 2017). It is these aspect of our findings and their consistency across animals and samples that make a compelling case for the possibility that a lethal viral infection of Zooxanthellae could be involved in the pathogenesis of SCTL D.

Another interpretation of our findings is that the anisometric VLP seen in chloroplasts are some form of degradation structures of this organelle secondary to heat stress or other undefined environmental insult. Indeed, SCTL D is thought to have originated near Miami harbor in 2014 in corals that were exposed to a combination of elevated temperatures (Precht et al. 2016) and sedimentation from dredging activities (Miller et al. 2016). However, structures observed here have not been documented by electron microscopy in Zooxanthellae of cnidaria exposed to particulate organic matter (Rosset et al. 2015), deprived of light (Muller-Parker et al. 1996), undergoing bleaching (Ladrière et al. 2008), undergoing nitrogen deprivation (Jiang et al. 2014), or exposed to UV and far red radiation (Camaya et al. 2016). The one exception was a study by Lohr et al. (2007) where cultured Zooxanthellae from an archived collection experimentally exposed to UV radiation showed intracytoplasmic cavities associated with AVLP in stellate configurations similar to Fig. 1D (arrow). However, in plants, AVLP are

not a feature of chloroplast degradation except for viral infections (Sowden et al. 2017), so it is difficult to explain the structures we saw as a byproduct of UV exposure in corals.

A viral infection killing Zooxanthellae would explain epidemiologic and anatomic features of SCTL. The disease appears to have originated near Miami harbor and spread north and south affecting multiple species of corals suggesting an infectious contagion (Muller et al. 2020). Histologic examination of diseased and healthy corals showed necrosis of Zooxanthellae and host cells affecting corals manifesting gross lesions of SCTL and apparently normal corals suggesting a widespread phenomenon (Landsberg et al. 2020). Zooxanthellae are the common denominator of all species of corals in the Caribbean where clades A and B dominate (Baker 2003), and a viral infection killing Zooxanthellae leading to host cell death and clinical manifestations of SCTL is a reasonable hypothesis based on findings herein. Perhaps Zooxanthellae clades A and B are particularly susceptible to viral infections in contrast to corals in the Pacific that are dominated by Clade C where lesions compatible with SCTL at the microscopic level have yet to be documented (Williams et al. 2010, Work and Aeby 2011, Work et al. 2012, Rodríguez-Villalobos et al. 2014, Work et al. 2014, Rodríguez-Villalobos et al. 2015, Work et al. 2015). Other aspects of SCTL would also accord with a virus infection of Zooxanthellae. Landsberg et al. (2020) found histologic lesions in corals that were apparently healthy, and like her, we saw Zooxanthellae pathology associated with AVLP in both healthy and lesioned corals suggesting that viral infection is widespread and enzootic. Treating lesion margins of corals affected with SCTL stops progression of disease but does not prevent genesis of new lesions (Shilling et al. 2021) fitting the pattern of a systemic virus disease affecting Zooxanthellae throughout the colony where virus-induced pathology could arise anywhere. An possible analogy would be smallpox in humans with multicentric lesions on the skin (Councilman 1905).

Reasons why a viral disease would appear in Zooxanthellae of Florida corals in 2014 and its origins are speculative. Zooxanthellae can move long distances. For instance, a new clade of Zooxanthellae was recently documented invading the Caribbean from the Pacific rendering infected corals there less susceptible to bleaching but making them poorer depositors of calcium carbonate (Pettay et al. 2015). A similar mechanism could be responsible for introduction of novel pathogens. Alternatively, this virus has been present historically in Florida, but somehow environmental conditions have changed sufficiently to allow it to flourish. For instance, climate change is expected to significantly alter the dynamics and spread of plant pathogens (Jones 2012), so conceivably, the same could apply to Zooxanthellae.

Logical next steps would be to confirm the presence of viral infections in Zooxanthellae through other means. Attempts to grow and propagate the virus in culture guided by light and electron microscopy would confirm whether lesions seen in the laboratory can replicate those seen here. It would also allow for a better understanding of viral morphogenesis and host response thus confirming or refuting our interpretation of putative developmental stages. Fortunately Zooxanthellae (Taguchi and Kinzie 2001) are more readily cultured than coral host cells (Helman et al. 2008), so this is a plausible objective. Identifying the virus through molecular means is also critical. Single stranded RNA viruses have been identified in corals in the Caribbean through molecular means, however, none of the viruses identified to date match the morphology of AVLP seen here (Correa et al. 2013). Molecular biology of plant viruses is a well-developed field (Roossinck et al. 2015), so deep sequencing to identify this virus is also a plausible objective. It would be imperative to localize the virus to the anatomic lesion through tools like in-situ hybridization or immunohistochemistry (Mochizuki and Ohki 2015), and fortunately, archived tissues exist to do this (Landsberg et al. 2020). Assessing whether SCTL can be reproduced in corals known to be AVLP negative would be important and would ease the development and validation of rapid diagnostic assays to detect the virus in the field. This would then permit a better understanding of the epidemiology of infections possibly setting the stage for management options and interventions.

5. Acknowledgments: My sincere thanks go to Tina Weatherby at the University of Hawaii Biological Electron Microscopy Core facility for preparation of TEM grids. Funding for this project was provided by the Florida Department of Environmental Protection through the Coral Protection and Restoration program (PO# B8E83B).

6. References

- Ackermann, H.-W., and K. L. Tiekotter. 2012. Murphy's law-if anything can go wrong, it will: Problems in phage electron microscopy. *Bacteriophage* **2**:122-129.
- Agrios, G. N. 2004. *Plant Pathology*. Elsevier, Netherlands.
- Baker, A. 2003. Flexibility and Specificity in Coral-Algal Symbiosis: Diversity, Ecology, and Biogeography of Symbiodinium. *Annual Review of Ecology, Evolution, and Systematics* **34**:661-689.
- Bhattacharyya, D., and S. Chakraborty. 2018. Chloroplast: the Trojan horse in plant-virus interaction. *Molecular plant pathology* **19**:504-518.
- Camaya, A. P., S. Sekida, and K. Okuda 2016. Changes in the Ultrastructures of the Coral *Pocillopora damicornis* after Exposure to High Temperature, Ultraviolet and Far-Red Radiation. *Cytologia* **81**:465-470.
- Correa, A. M. S., R. M. Welsh, and R. L. V. Thurber. 2013. Unique nucleocytoplasmic dsDNA and +ssRNA viruses are associated with the dinoflagellate endosymbionts of corals. *The ISME Journal* **7**:13-27.
- Councilman, W. T. 1905. Some General Considerations on the Pathology of Smallpox. *Public health papers and reports* **31**:218-229.
- Davy, J. E., and N. L. Patten. 2007. Morphological diversity of virus-like particles within the surface microlayer of scleractinian corals. *Aquatic Microbial Ecology* **47**:37-44.
- Davy, S. K., S. G. Burchett, A. L. Dale, P. Davies, J. E. Davy, C. Muncke, O. Hoegh-Guldberg, and W. H. Wilson. 2006. Viruses: agents of coral disease? *Diseases of Aquatic Organisms* **69**:101-110.
- Glibert, P. M., and J. M. Burkholder. 2018. Causes of Harmful Algal Blooms. Pages 1-38 *Harmful Algal Blooms*.
- Harrison, F. W., and E. A. Ruppert. 1990. *Microscopic Anatomy of Invertebrates*. Volume 2: Placozoa, Porifera, Cnidaria, and Ctenophora. Wiley-Liss, New York.
- Helman, Y., F. Natale, R. Sherrell, M. LaVigne, V. Starovoytov, M. Gorbunov, and P. Falkowski. 2008. Extracellular matrix production and calcium carbonate precipitation by coral cells in vitro. *Proceedings of the National Academy of Sciences* **105**:54-58.
- Jiang, P.-L., B. Pasaribu, and C.-S. Chen. 2014. Nitrogen-Deprivation Elevates Lipid Levels in Symbiodinium spp. by Lipid Droplet Accumulation: Morphological and Compositional Analyses. *PLOS One* **9**:e87416.
- Jones, R. 2012. Influence of climate change on plant disease infections and epidemics caused by viruses and bacteria. *CAB Reviews: Perspectives in Agriculture, Veterinary Science, Nutrition and Natural Resources* **7**.
- Ladrière, O., P. Compère, D. Nicole, P. Vandewalle, and M. Poulicek. 2008. Morphological alterations of zooxanthellae in bleached cnidarian hosts. *Cahiers de Biologie Marine* **49**:215-227.
- Landsberg, J. H., Y. Kiryu, E. C. Peters, P. W. Wilson, N. Perry, Y. Waters, K. E. Maxwell, L. K. Huebner, and T. M. Work. 2020. Stony Coral Tissue Loss Disease in Florida Is Associated With Disruption of Host-Zooxanthellae Physiology. *Frontiers in Marine Science* **7**:1090.
- Lohr, J., C. Munn, and W. Wilson. 2007. Characterization of a Latent Virus-Like Infection of Symbiotic Zooxanthellae. *Applied and Environmental Microbiology* **73**:2976-2981.
- McWhorter, F. P. 1965. Plant Virus Inclusions. *Annual Review of Phytopathology* **3**:287-312.

- Miller, M. W., J. Karazsia, C. E. Groves, S. Griffin, T. Moore, P. Wilber, and K. Gregg. 2016. Detecting sedimentation impacts to coral reefs resulting from dredging the Port of Miami, Florida USA. *PeerJ* **4**:e2711.
- Mochizuki, T., and S. T. Ohki. 2015. Detection of Plant Virus in Meristem by Immunohistochemistry and In Situ Hybridization. Pages 275-287 in I. Uyeda and C. Masuta, editors. *Plant Virology Protocols. Methods in Molecular Biology (Methods and Protocols)*, Humana Press, New York, NY.
- Muller-Parker, G., K. W. Lee, and C. B. Cook. 1996. Changes in the ultrastructure of symbiotic zooxanthellae (*Symbiodinium* sp., dinophyceae) in fed and starved sea anemones maintained under high and low light. *Journal of Phycology* **32**:987-994.
- Muller, E. M., C. Sartor, N. I. Alcaraz, and R. van Woesik. 2020. Spatial Epidemiology of the Stony-Coral-Tissue-Loss Disease in Florida. *Frontiers in Marine Science* **7**.
- Neely, K. L., K. A. Macaulay, E. K. Hower, and M. A. Dobler. 2020. Effectiveness of topical antibiotics in treating corals affected by Stony Coral Tissue Loss Disease. *PeerJ* **8**:e9289.
- Netherton, C., K. Moffat, E. Brooks, and T. Wileman. 2007. A guide to viral inclusions, membrane rearrangements, factories, and viroplasm produced during virus replication. *Adv Virus Res* **70**:101-182.
- Pettay, D. T., D. C. Wham, R. T. Smith, R. Iglesias-Prieto, and T. C. LaJeunesse. 2015. Microbial invasion of the Caribbean by an Indo-Pacific coral zooxanthella. *Proceedings of the National Academy of Sciences* **112**:7513.
- Precht, W. F., B. E. Gintert, M. L. Robbart, R. Fura, and R. van Woesik. 2016. Unprecedented Disease-Related Coral Mortality in Southeastern Florida. *Scientific Reports* **6**:31374.
- Rodríguez-Villalobos, J. C., A. Rocha-Olivares, T. M. Work, L. E. Calderon-Aguilera, and J. A. Cáceres-Martínez. 2014. Gross and microscopic pathology of lesions in *Pocillopora* spp. from the subtropical eastern Pacific. *Journal of Invertebrate Pathology* **120**:9-17.
- Rodríguez-Villalobos, J. C., T. M. Work, L. E. Calderon-Aguilera, H. Reyes-Bonilla, and L. Hernández. 2015. Explained and unexplained tissue loss in corals from the Tropical Eastern Pacific. *Diseases of Aquatic Organisms* **116**:121-131.
- Roossinck, M. J., D. P. Martin, and P. Roumagnac. 2015. Plant Virus Metagenomics: Advances in Virus Discovery. *Phytopathology*® **105**:716-727.
- Rosales, S. M., A. S. Clark, L. K. Huebner, R. R. Ruzicka, and E. M. Muller. 2020. Rhodobacterales and Rhizobiales Are Associated With Stony Coral Tissue Loss Disease and Its Suspected Sources of Transmission. *Frontiers in microbiology* **11**.
- Rosset, S., C. D'Angelo, and J. Wiedenmann. 2015. Ultrastructural Biomarkers in Symbiotic Algae Reflect the Availability of Dissolved Inorganic Nutrients and Particulate Food to the Reef Coral Holobiont. *Frontiers in Marine Science* **2**.
- Shilling, E. N., I. R. Combs, and J. D. Voss. 2021. Assessing the effectiveness of two intervention methods for stony coral tissue loss disease on *Montastraea cavernosa*. *Scientific Reports* **11**:8566.
- Sowden, Robert G., Samuel J. Watson, and P. Jarvis. 2017. The role of chloroplasts in plant pathology. *Essays in Biochemistry* **62**:21-39.
- Stevens, W. A. 1983. Plant Virus Structure. Pages 69-93 *Virology of Flowering Plants*. Springer, Boston, MA.
- Taguchi, S., and R. A. Kinzie Iii. 2001. Growth of zooxanthellae in culture with two nitrogen sources. *Marine Biology* **138**:149-155.
- Taylor, D. L. 1968. In situ studies on the cytochemistry and ultrastructure of a symbiotic marine dinoflagellate. *Journal of the Marine Biological Association of the United Kingdom* **48**:349-366.
- Trench, R. K., and R. J. Blank. 1987. *Symbiodinium microadriaticum* freudenthal, *S. goreauii* sp. nov., *S. kawagutii* sp. nov. and *S. pilosum* sp. nov.: gymnodinioid dinoflagellate symbionts of marine *Journal of Phycology* **23**:469-481.

- Vega Thurber, R. L., and A. M. Correa. 2011. Viruses of reef-building scleractinian corals. *Journal of Experimental Marine Biology and Ecology* **408**:102-113.
- Weng, L.-C., B. Pasaribu, I. Ping Lin, C.-H. Tsai, C.-S. Chen, and P.-L. Jiang. 2014. Nitrogen Deprivation Induces Lipid Droplet Accumulation and Alters Fatty Acid Metabolism in Symbiotic Dinoflagellates Isolated from *Aiptasia pulchella*. *Scientific Reports* **4**:5777.
- Williams, G. J., T. M. Work, G. S. Aeby, I. S. Knapp, and S. K. Davy. 2010. Gross and microscopic morphology of lesions in Cnidaria from Palmyra Atoll, Central Pacific. *Journal of Invertebrate Pathology* **106**:165-170.
- Wilson, W. H., A. L. Dale, J. E. Davy, and S. K. Davy. 2005. An enemy within? Observations of virus-like particles in reef corals. *Coral Reefs* **24**:145-148.
- Wilson, W. H., I. Francis, K. Ryan, and S. K. Davy. 2001. Temperature induction of viruses in symbiotic dinoflagellates. *Aquatic Microbial Ecology* **25**:99-102.
- Work, T. M., and G. S. Aeby. 2011. Pathology of tissue loss (white syndrome) in *Acropora* sp. corals from the Central Pacific. *Journal of Invertebrate Pathology* **107**:127-131.
- Work, T. M., G. S. Aeby, and K. Huguen. 2015. Gross and microscopic pathology of corals from Micronesia. *Veterinary Pathology* **53**:153-162.
- Work, T. M., G. S. Aeby, G. Lasne, and A. Tribollet. 2014. Gross and microscopic pathology of hard and soft corals in New Caledonia. *Journal of Invertebrate Pathology* **120**:50-58.
- Work, T. M., J. Dagenais, T. M. Weatherby, G. H. Balazs, and M. Ackermann. 2017. In Vitro Replication of Chelonid Herpesvirus 5 in Organotypic Skin Cultures from Hawaiian Green Turtles (*Chelonia mydas*). *Journal of Virology* **91**.
- Work, T. M., R. Russell, and G. S. Aeby. 2012. Tissue loss (white syndrome) in the coral *Montipora capitata* is a dynamic disease with multiple host responses and potential causes. *Proceedings of Royal Society B* **279**:4334-4341.
- Yang, X., T. Zhang, B. Chen, and G. Zhou. 2017. Transmission Biology of Rice Stripe Mosaic Virus by an Efficient Insect Vector *Recilia dorsalis* (Hemiptera: Cicadellidae). *Frontiers in microbiology* **8**.
- Yellowlees, D., T. A. V. Rees, and W. Leggat. 2008. Metabolic interactions between algal symbionts and invertebrate hosts. *Plant, Cell & Environment* **31**:679-694.
- Zhao, J., X. Zhang, Y. Hong, and Y. Liu. 2016. Chloroplast in Plant-Virus Interaction. *Frontiers in microbiology* **7**.
- Zhu, B., K. Pan, and G. Wang. 2011. Effects of host starvation on the symbiotic dinoflagellates from the sea anemone *Stichodactyla mertensii*. *Marine Ecology* **32**:15-23.

Table 1. List of samples submitted to HFS for TEM partitioned by location, date of collection, species, ID, Presence or absence of lesions on histology, year submitted to HFS, and whether (Y) or not (N) TEM was done on the sample. MCAV, OFAV, CNAT, PSTR, SSID are acronyms for *Montastraea cavernosa*, *Orbicella faveolata*, *Colpophyllia natans*, *Pseudodiploria strigosa* and *Siderastrea siderea*.

Location	Date	Species	ID	Status	Lesion	Year	TEM
West Turtle Shore	4/10/2018	MCAV	320D	SCTLD-Lesion	YES	2020	Y
West Turtle Shore	4/10/2018	MCAV	319U	SCTLD-Healthy	NO	2020	Y
West Turtle Shore	4/10/2018	OFAV	308D	SCTLD-Lesion	YES	2020	Y
West Turtle Shore	4/10/2018	OFAV	308U	SCTLD-Healthy	YES	2020	Y
West Turtle Shore	4/10/2018	SSID	325D	SCTLD-Lesion	YES	2020	N
West Turtle Shore	4/10/2018	SSID	325U	SCTLD-Healthy	NO	2020	N
West Turtle Shore	4/9/2018	CNAT	300D	SCTLD-Lesion	YES	2020	Y
West Turtle Shore	4/9/2018	CNAT	300U	SCTLD-Healthy	NO	2020	Y
BOOT KEY	4/11/2018	PSTR	375D	SCTLD-Lesion	YES	2020	Y
BOOT KEY	4/11/2018	PSTR	375U	SCTLD-Healthy	NO	2020	Y
SITE F-reference	5/8/2018	MCAV	506H	Healthy	NO?	2020	Y
SITE F-reference	5/8/2018	PSTR	512H	Healthy	NO?	2020	Y
SITE F-reference	5/8/2018	OFAV	503H	Healthy	NO?	2020	Y
SITE F-reference	5/8/2018	SSID	509H	Healthy	NO?	2020	Y
SITE F-reference	5/8/2018	CNAT	516H	Healthy	NO?	2020	Y
West Turtle Shore	4/10/2018	MCAV	317U	SCTLD-Healthy	NO HISTO	2021	Y
West Turtle Shore	4/10/2018	MCAV	318D	SCTLD-Lesion	NO HISTO	2021	Y
West Turtle Shore	4/10/2018	MCAV	318U	SCTLD-Healthy	NO HISTO	2021	Y
West Turtle Shore	4/9/2018	OFAV	310D	SCTLD-Lesion	NO	2021	Y
West Turtle Shore	4/9/2018	OFAV	310U	SCTLD-Healthy	NO	2021	Y
West Turtle Shore	4/10/2018	SSID	324U	SCTLD-Healthy	NO	2021	Y
West Turtle Shore	4/10/2018	SSID	327D	SCTLD-Lesion	NO HISTO	2021	Y
BOOT KEY	4/11/2018	CNAT	342D	SCTLD-Lesion	YES	2021	Y
BOOT KEY	4/11/2018	CNAT	342U	SCTLD-Healthy	NO	2021	Y
West Turtle Shore	4/9/2018	PSTR	332U	SCTLD-Healthy	NO HISTO	2021	Y
BOOT KEY	4/11/2018	PSTR	376D	SCTLD-Lesion	NA	2021	Y
BOOT KEY	4/11/2018	PSTR	376U	SCTLD-Healthy	NO	2021	Y

Table 2. Number of photomicrographs (number of individual Zooxanthellae) partitioned by health status of fragment and genus.

Genus	SCTLD-Lesion	SCTLD-Healthy	Healthy	Grand Total
<i>Colpophyllia</i>	136 (52)	152 (12)	20 (76)	308 (140)
<i>Montastraea</i>	100 (37)	202 (29)	60 (78)	362 (144)
<i>Orbicella</i>	105 (26)	152 (29)	87 (55)	344 (110)
<i>Pseudodiploria</i>	136 (63)	181 (21)	60 (67)	377 (151)
<i>Siderastrea</i>	126 (33)	73 (47)	186 (19)	385 (99)
Grand Total	603 (211)	760 (138)	413 (295)	1776 (644)

Figure 1. A) *Siderastrea* SCTL D-Healthy. Normal Zooxanthellae with pyrenoid (p) and annular starch (s), starch granules (white arrow), nucleus (n), multilobulated chloroplasts with distinct thylakoid membranes (arrowhead). B) *Montastraea* SCTL D-Healthy. Gigantism of chloroplasts (g); note massive enlargement and lack of detail of thylakoid membranes, lack of starch granules, and lack of pyrenoid. C) *Pseudodiploria* SCTL D-Healthy. Cavity (asterisk) and electron dense amorphous matrix (arrow). D) *Orbicella* SCTL D-Healthy. Cavity (asterisk) with debris; E) *Pseudodiploria* SCTL D-Lesion. Whorled electron dense material (arrow) streaming from electron dense viroplasm within cavity. F) Detail of E; note putative early stage anisometric viral like particles (arrow).

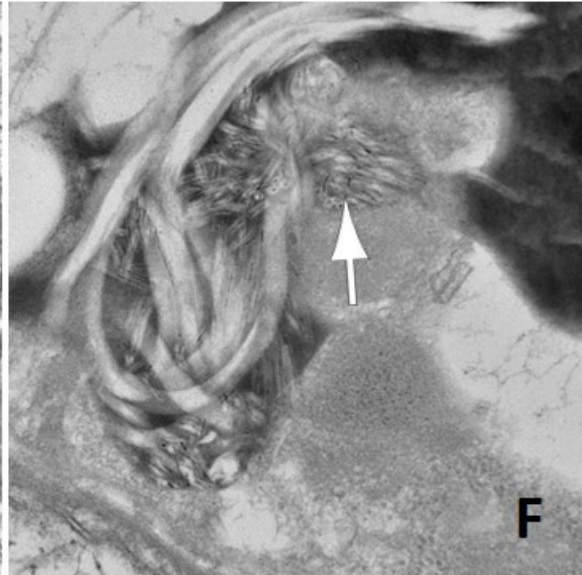
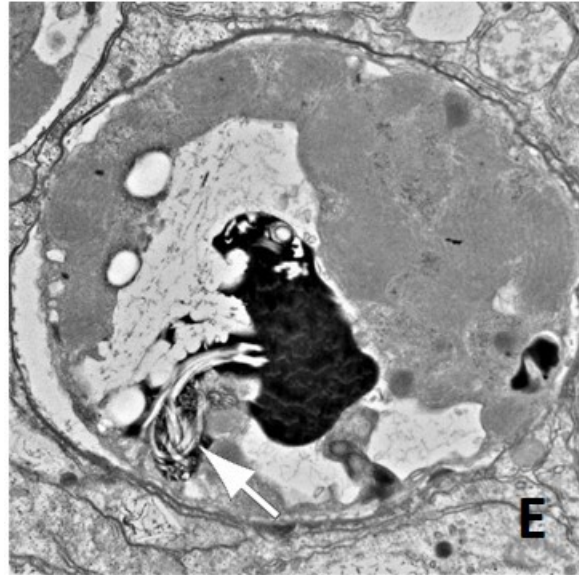
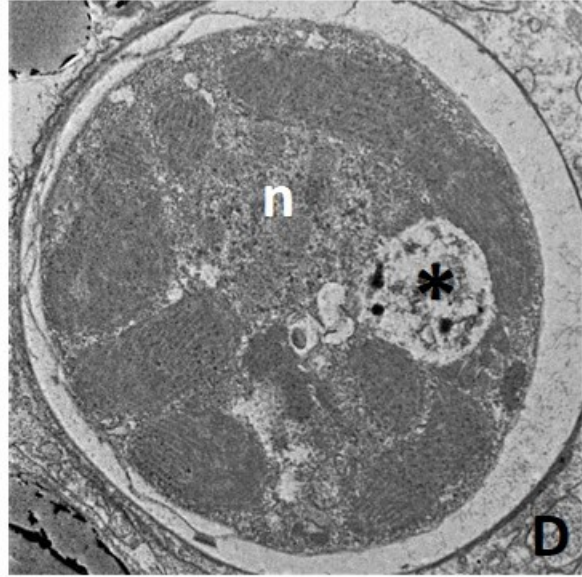
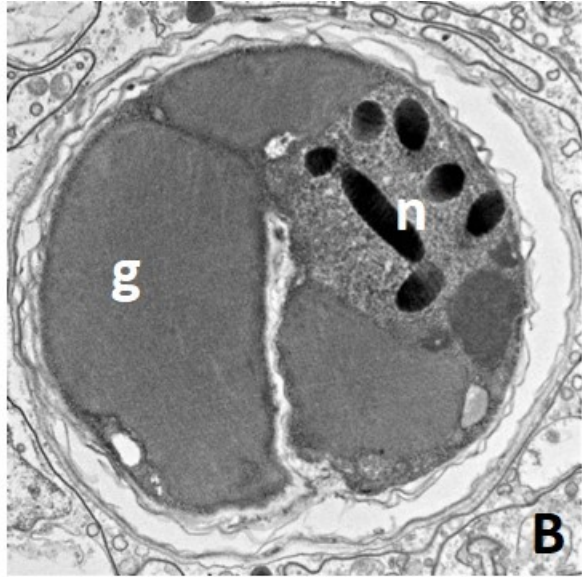
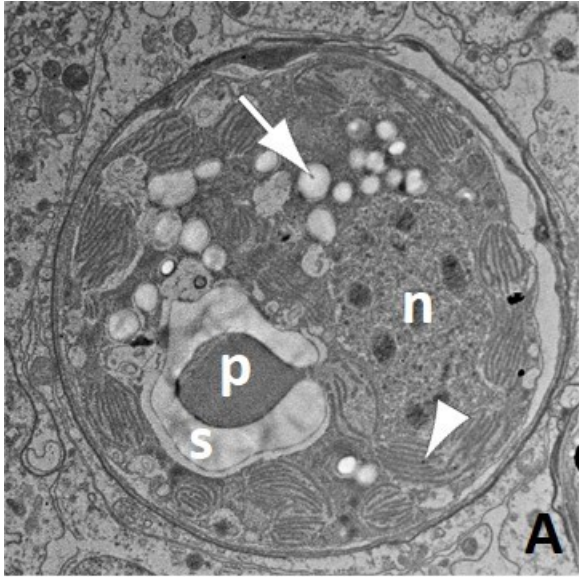


Figure 2. A) *Colpophyllia* SCTL D-Lesion. Putative early inclusion of anisometric viral like particles (AVLP) within chloroplasts (arrow). B) Detail of A, note arrays of sinuous AVLP (arrow) mixed with electron dense material and cross sections with a core (arrowhead). C) *Orbicella* SCTL D-Healthy. Putative intermediate stage of viral infection; note large cavity containing clumps of electron dense material and clusters of coarse AVLP arranged in stellate (arrow) and haphazard (arrowhead) pattern. D) Detail of C; note cluster of stellate AVLP (arrow) and coarser haphazardly arranged AVLP admixed with clumps of electron dense material. E) *Colpophyllia* SCTL D-Healthy. Putative advanced stage of viral infection; note cavity containing clumps of electron dense material mixed with AVLP arranged in stellate (arrow) or haphazard manner (arrowhead). F) Detail of haphazardly arranged AVLP; note core in saggital (arrow) and cross (arrowhead) sections of individual AVLP.

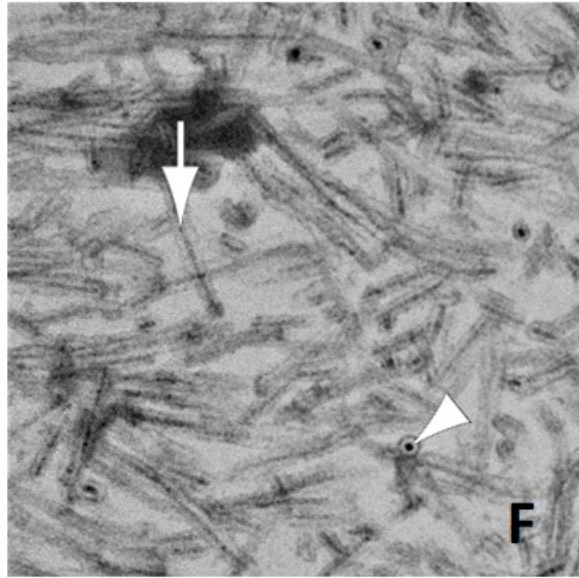
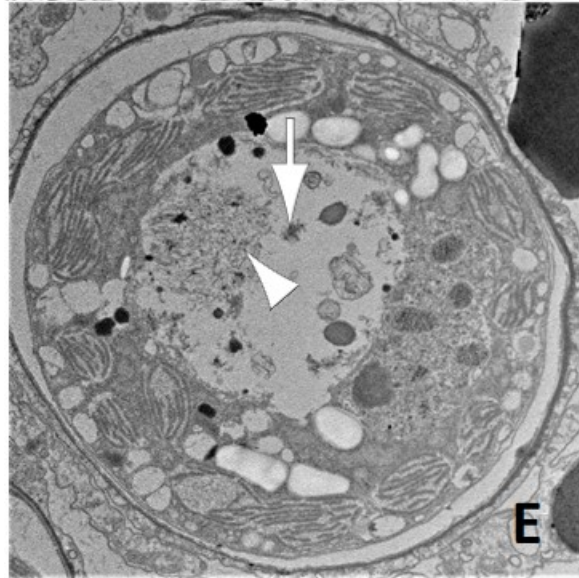
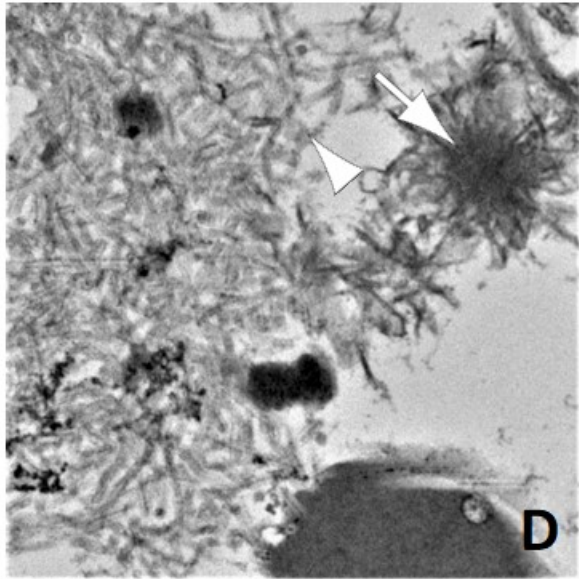
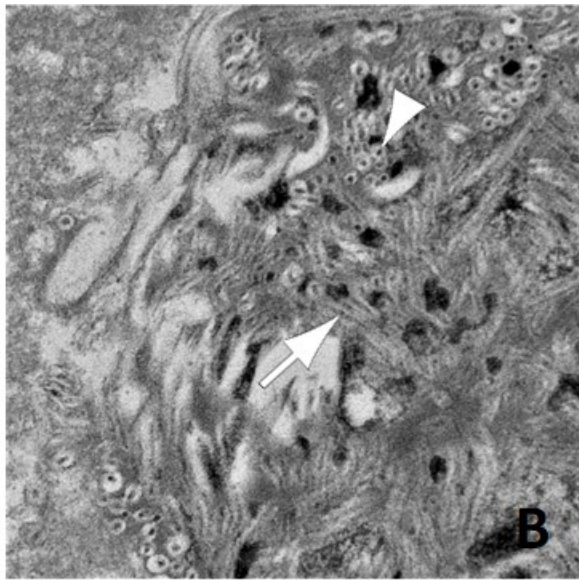
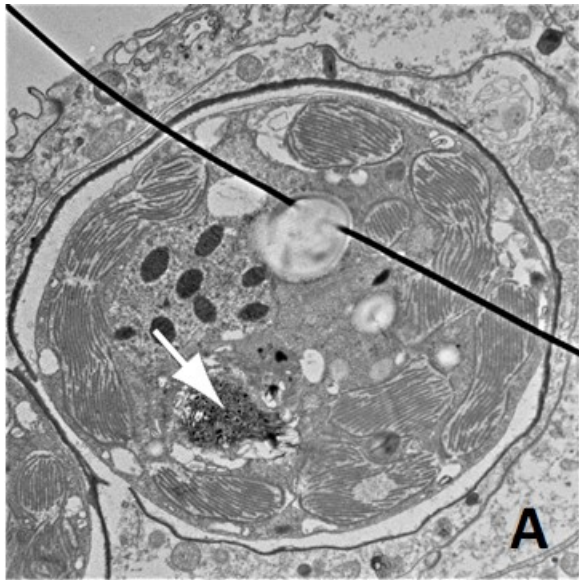


Figure 3. A) *Colpophyllia* SCTL D-Healthy; detail of viroplasm (v) with formation of anisometric viral like particle (AVLP-arrow). B) *Montastraea* SCTL D-Healthy; note laminated membranes (arrowhead) associated with haphazardly arranged AVLP (arrow). C) *Colpophyllia* SCTL D-Lesion; Note large cavity with electron dense material suggestive of viroplasm (v). D) Close up of A with viroplasm (v), cluster of stellate AVLP (arrow) and membrane formation (arrowhead). E) *Colpophyllia*-SCTL D-Healthy; Note viroplasm (v) surrounded by numerous haphazardly arranged coarse AVLP. F) *Colpophyllia* SCTL D-Healthy; More electron dense viroplasm (v) out of which appear to arise AVLP visible in longitudinal (arrow) and cross (arrowhead) sections.

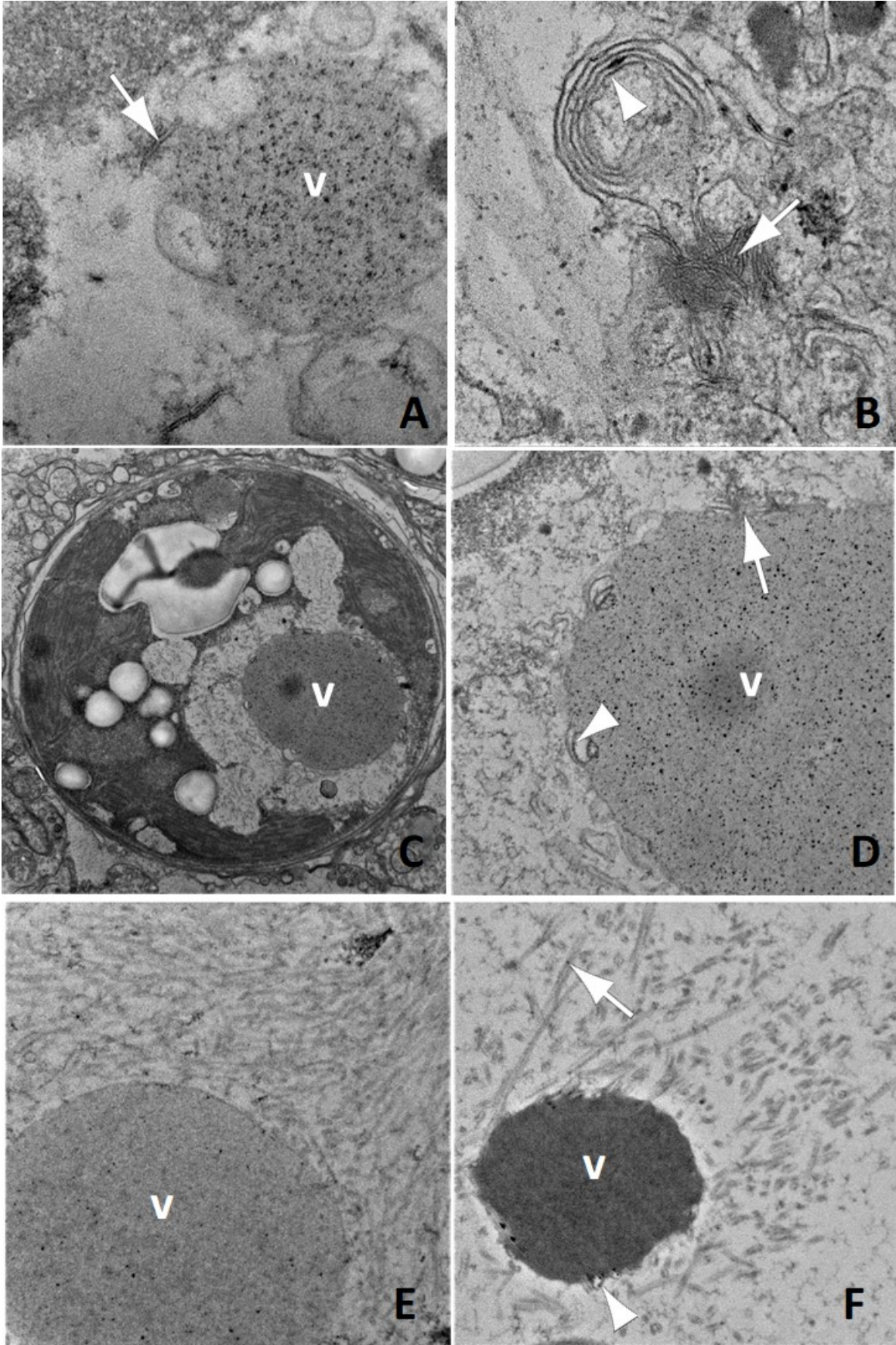


Figure 4. A) *Montastraea* SCTLD-Healthy. Putative late stage infection; note large cavity effacing most of the cellular architecture and replete with electron dense material, membranes (arrowhead and anisometric viral like particles (AVLP-arrow). B) Detail of A; note AVLP arrayed in lamina (arrow). C) *Pseudodiploria* SCTLD-Healthy. Large inclusion of coarse AVLP arrayed haphazardly (arrow) mixed with electron dense material associated with lysis of cell wall (asterisk). D) Detail of C; note AVLP (arrow). E) *Pseudodiploria*-SCTLD Healthy. Lysed cell; note large pleomorphic cavity with abundant debris and loss of membrane integrity with clumps of tubular structures (arrow). F) Detail of E.

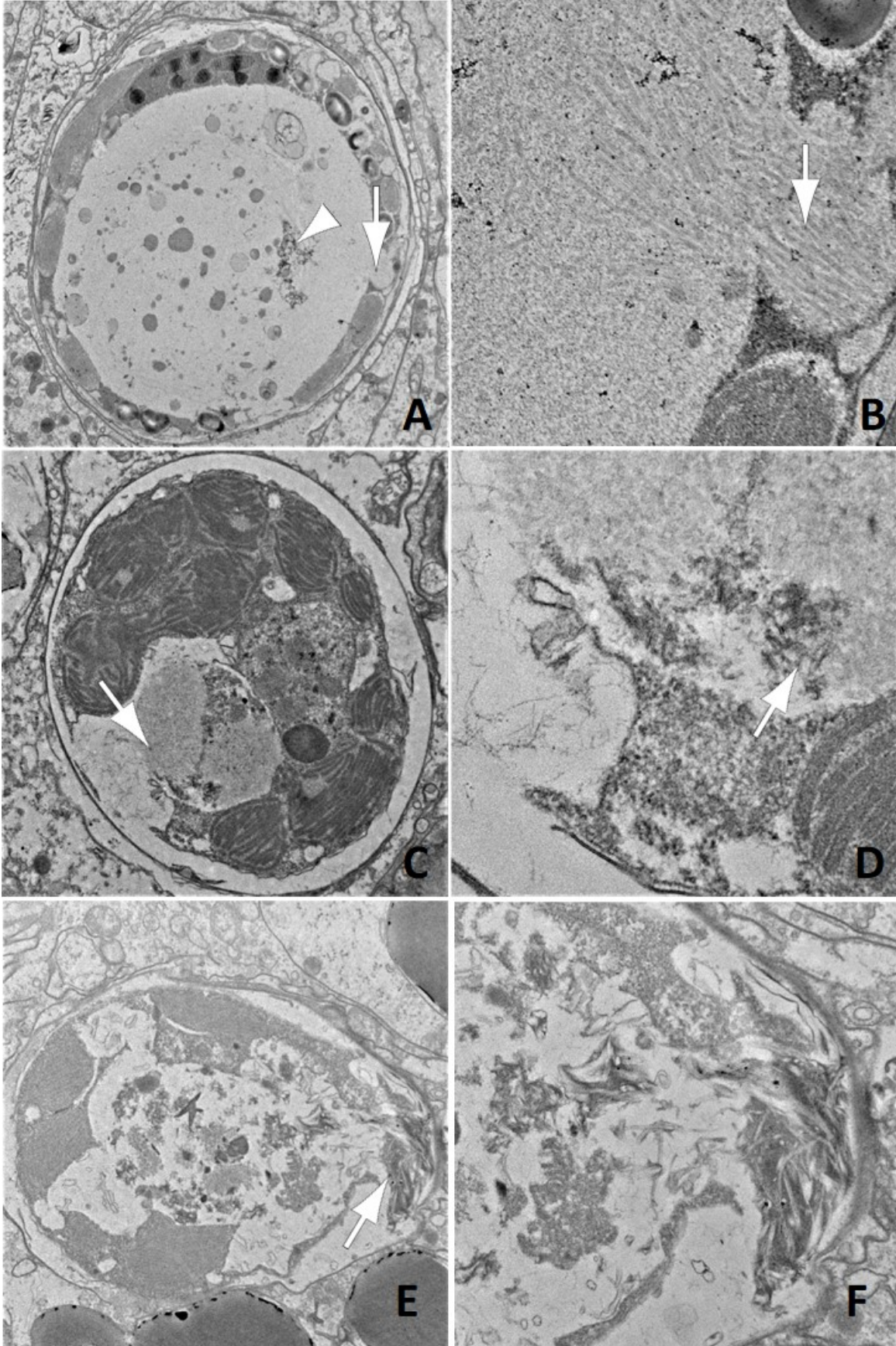


Figure 5. Percent of Zooxanthellae having fine anisometric viral like particles (AVLP) or black whorls partitioned by health state and genus. SCTLD-H and SCTLD-L refer to fragments from diseased colonies without and with lesions.

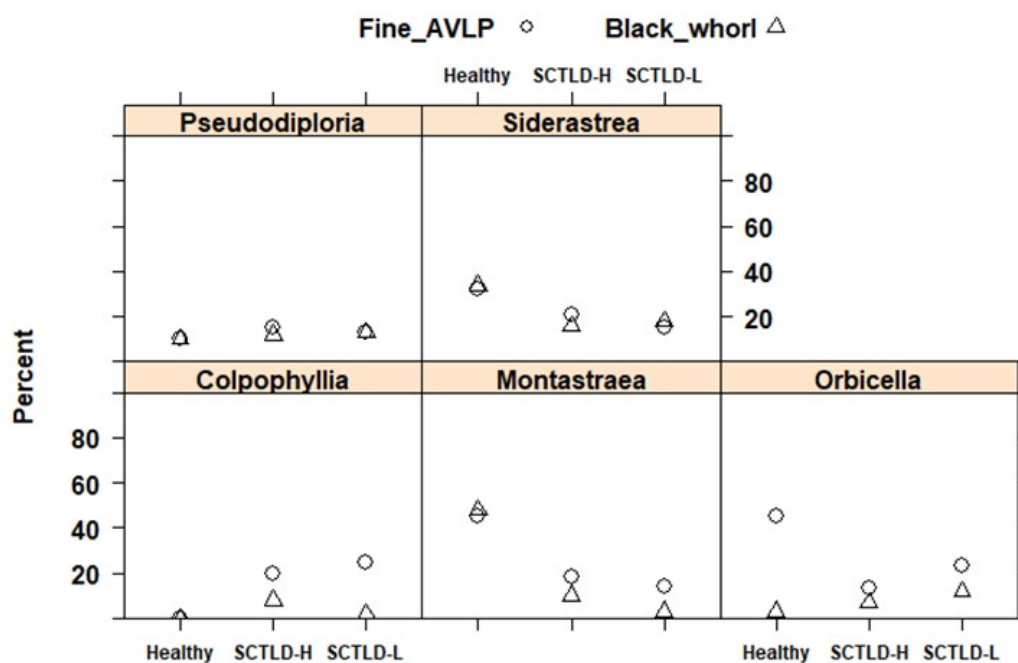


Figure 6. Percent of Zooxanthellae having fine stellate or coarse anisometric viral like particles (AVLP) partitioned by health state and genus. SCTLD-H and SCTLD-L refer to fragments from diseased colonies without and with lesions.

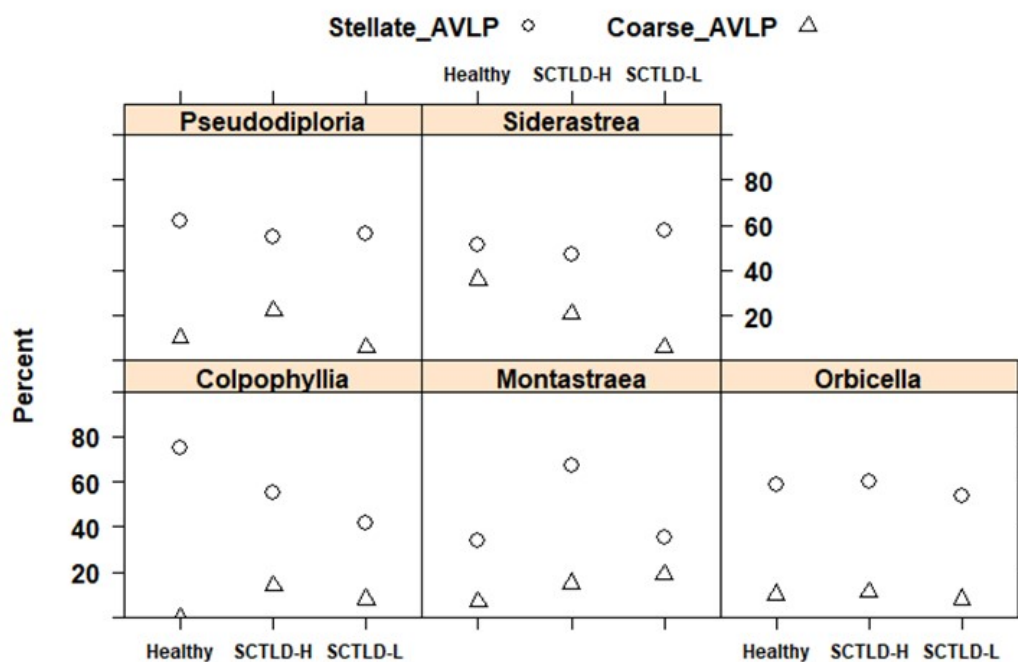


Figure 7. Percent of Zooxanthellae having absence of pyrenoid starch or starch granules partitioned by fragment health state and coral genus. SCTLD-H and SCTLD-L refer to fragments from diseased colonies without and with lesions.

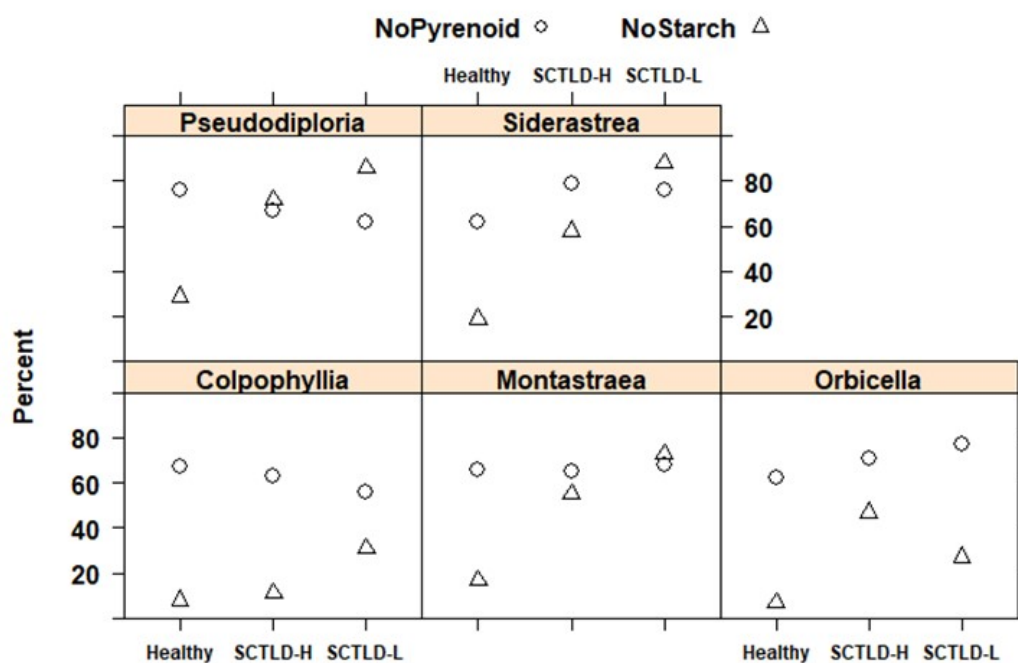


Figure 8. Percent of Zooxanthellae having intracellular cavities or electron dense amorphous material partitioned by fragment health state and coral genus. SCTLD-H and SCTLD-L refer to fragments from diseased colonies without and with lesions.

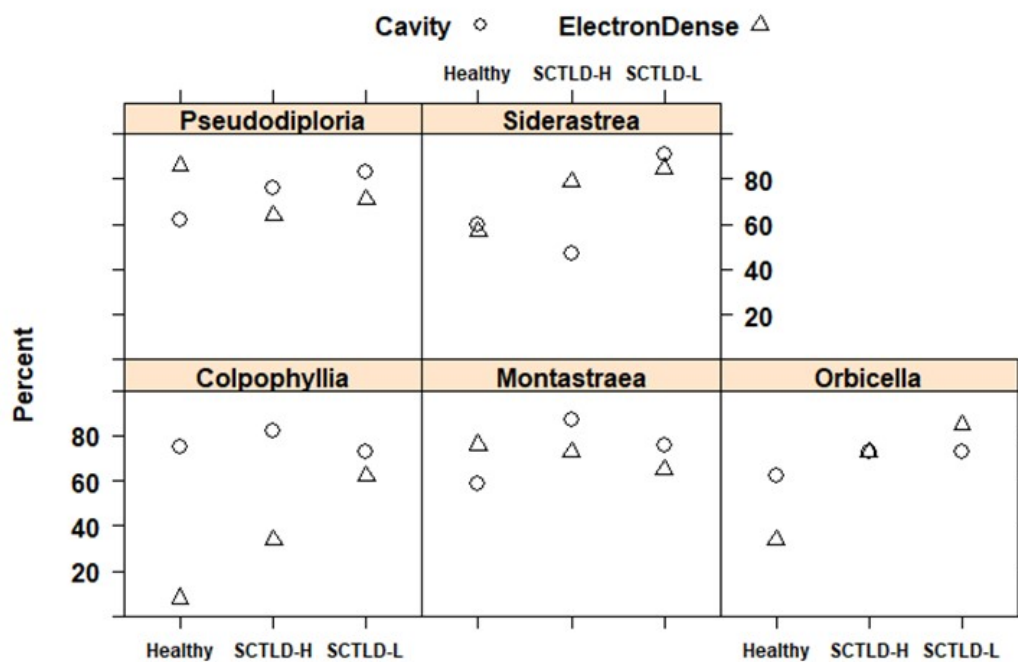


Figure 9. Percent of Zooxanthellae having indistinct thylakoid membranes (TM) or gigantism of chloroplasts partitioned by health state and genus. SCTLD-H and SCTLD-L refer to fragments from diseased colonies without and with lesions.

